(*1*). The rostral portion of the *Rhamphorhynchus* species differs from that of *Thalassodromeus* because it is toothed, is comparatively reduced, and has a less sharp and smaller anterior rostral projection. Furthermore, the skull in *Rhamphorhynchus* lacks the adaptations for skimming activity discussed above and might have had only crude and limited skimming behavior. Another difference between both is size. Although most *Rhamphorhynchus* specimens have a wingspan ranging from 500 to 1200 mm [the largest one being 1750 mm (*31*)], the estimated length represented by the type material of *Thalassodromeus sethi* [based on other tapejarid specimens (*8*, *22*)] varies between 4200 and 4500 mm, making it a large volant creature that got its nourishment by skimming the Araripe lagoon and the nearby ocean 110 million years ago.

References and Notes

1. P. Wellnhofer, *The Illustrated Encyclopedia of Pterosaurs* (Salamander, London, 1991).
2. A. W. A. Kellner, *Acta Geol. Leopoldensia* **39**, 175 (1994).
3. G. Beurlen, *An. Acad. Bras. Cienc. Suppl.* **43**, 411 (1971).
4. J. G. Maisey, Ed., *Santana Fossils, An Illustrated Atlas* (T. F. H. Publishers, Neptune City, NJ, 1991).
5. D. Pons, P. Y. Berthou, D. A. Campos, in *Atas 1: Simpósio da Bacia Araripe e Bacias Interiores do Nordeste*, D. A. Campos, M. S. S. Viana, Eds. (Crato, Ceará, Brasil, 1990), pp. 241–252.
6. E. Frey, D. Martill, *Neues Jahrb. Geol. Palaeontol. Abh.* **194**, 379 (1994).
7. D. A. Campos, A. W. A. Kellner, *An. Acad. Bras. Cienc.* **69**, 83 (1997).
8. J. M. Sayão, A. W. A. Kellner, *Bol. Museu Nacional Geologia* **54**, 1 (2000).
9. L. I. Price, *An. Acad. Bras. Cienc. Suppl.* **43**, 451 (1971).
10. P. Wellnhofer, *Palaeontographica* **187**, 105 (1985).
11. D. A. Campos, A. W. A. Kellner, *An. Acad. Bras. Cienc.* **57**, 453 (1985).
12. A. W. A. Kellner, Y. Tomida, *Nat. Sci. Museum Monogr.* **17**, 1 (2000).
13. A. W. A. Kellner, W. Langston, *J. Vertebr. Paleontol.* **16**, 222 (1996).
14. A. W. A. Kellner, *An. Acad. Bras. Cienc.* **61**, 439 (1989).
15. P. Wellnhofer, A. W. A. Kellner, *Mitt. Bayer. Staatsslg. Palaeontol. Hist. Geol.* **31**, 89 (1991).
16. G. F. Eaton, *Mem. Conn. Acad. Arts Sci.* **2**, 1 (1910).
17. C. S. Bennett, *Palaeontographica* **260**, 1 (2001).
18. C. C. Young, *Spec. Publ. Inst. Vert. Paleontol. Paleoanthr. Acad. Sin.* **11**, 18 (1973) (in Chinese).
19. A. W. A. Kellner, thesis, Columbia University (1996).
20. _____, D. A. Campos, *An. Acad. Bras. Cienc.* **60**, 459 (1988).
21. _____, *An. Acad. Bras. Cienc.* **66**, 467 (1994).
22. A. W. A. Kellner, Y. Hasegawa, *J. Vertebr. Paleontol.* **13** (suppl. to 3), 44A (1993).
23. E. Buffetaut, D. Grigorescu, Z. Csiki, *Naturwissenschaften* **89**, 180 (2002).
24. J. O. Farlow, C. V. Thompson, D. E. Rosner, *Science* **192**, 1123 (1976).
25. S. Sampson, *Dinofest Intern. Proc.* **1997**, 39 (1997).
26. W. Langston, *Sci. Am.* **244**, 122 (1981).
27. S. C. Bennett, *J. Vertebr. Paleontol.* **12**, 422 (1992).
28. D. Kripp, *Nova Acta Leopold. N. F.* **12**, 16 (1943).
29. C. D. Bramwell, G. R. Whitfield, *Philos. Trans. R. Soc. London Ser. B* **267**, 503 (1981).
30. R. Zusi, *Publ. Nuttall Ornithol. Club* **3**, 1 (1962).
31. P. Wellnhofer, *Palaeontographica* **148**, 1 (1975).

32. We thank V. Arraes de Alencar Gervaiseau, P. Nuvens, Á. Saravaia (Universidade Regional do Cariri), and A. Andrade (Departamento Nacional de Produção Mineral, Crato) for supporting fieldwork at the Araripe Basin; J. de Alencar (Crato) for assisting D.A.C. during field activities; J. G. Maisey, G. Leonardi, G. Ligabue, and P. Taquet for discussions about this specimen; H. Silva and M. Craik (MN/UFRJ) for helping with the preparation of the material; and M. Oliveira (MN/UFRJ) for the drawings used in this paper. Partially funded by the Fundação Carlos Chagas de Amparo à Pesquisa do Rio de Janeiro.

Supporting Online Material
www.sciencemag.org/cgi/content/full/297/5580/389/DC1
Figs. S1 and S2

23 April 2002; accepted 14 June 2002

Generation and in Vitro Differentiation of a Spermatogonial Cell Line

Li-Xin Feng,[1] Yali Chen,[1] Luis Dettin,[1] Renee A. Reijo Pera,[2] John C. Herr,[3] Erwin Goldberg,[4] Martin Dym[1]

Spermatogenesis is the process by which spermatogonial stem cells divide and differentiate to produce sperm. In vitro sperm production has been difficult to achieve because of the lack of a culture system to maintain viable spermatogonia for long periods of time. Here we report the in vitro generation of spermatocytes and spermatids from telomerase-immortalized mouse type A spermatogonial cells in the presence of stem cell factor. This differentiation can occur in the absence of supportive cells. The immortalized spermatogonial cell line may serve as a powerful tool in elucidating the molecular mechanisms of spermatogenesis. Furthermore, through genomic modification and transplantation techniques, this male germ cell line may be used to generate transgenic mice and to develop germ cell gene therapy.

Spermatogonia originate from primordial germ cells (PGCs), which are derived from the epiblast by 7.5 days post coitum (dpc) and migrate through the dorsal mesentery and enter the developing fetal gonad, the genital ridge, between 10.5 and 12.5 dpc (*1*, *2*). Once

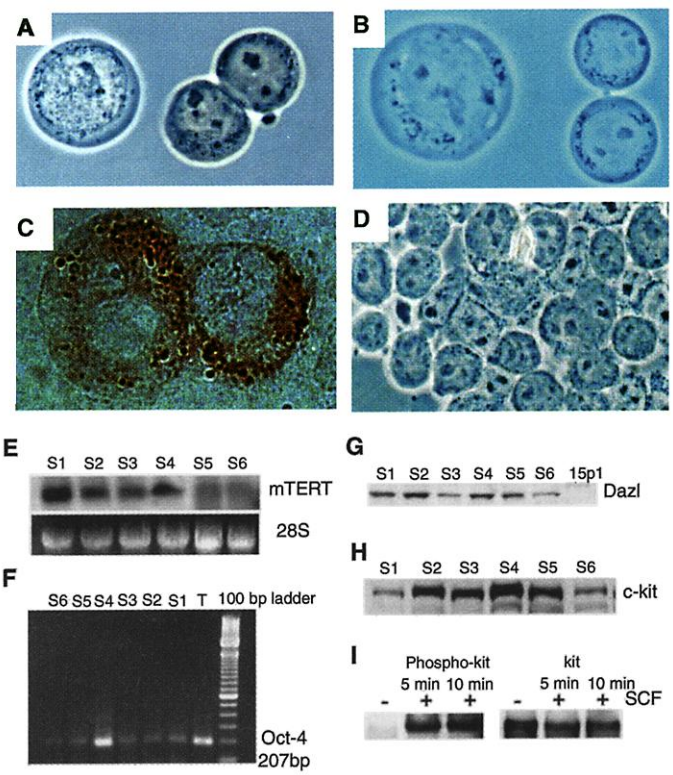

Fig. 1. Characterization of type A spermatogonial cell line. (**A**) After 2 months of culture, the immortalized cells displayed the typical morphology of type A spermatogonia, such as spherical nuclei and organelles in a perinuclear location. (**B**) Morphology of freshly isolated type A spermatogonia (control). (**C**) The immortalized cells were positive for c-kit, as shown by immunocytochemistry. (**D**) After subcloning and culture for 1 year, the immortalized cells still maintained the morphology of type A spermatogonia. (**E**) Northern blot (25 μg of total RNA for each lane) showing mTERT expression in cell lines S1 to S6. (**F**) Expression of Oct-4 in immortalized cells, shown by RT-PCR as a 207-bp product; lane T, control testis from newborn pups. (**G**) Dazl was expressed in all six cell clones, as shown by Western blot; the 15p-1 Sertoli cell line is a negative control. (**H**) c-kit was expressed in all six cell clones, as shown by Western blot. (**I**) After stimulation with mSCF (100 ng/ml) for 5 and 10 min, c-kit immunoprecipitates were probed for phosphotyrosine and reprobed for c-kit.

they arrive in the genital ridge, the PGCs are enclosed by somatic Sertoli cells and become prospermatogonia or gonocytes (*3*). The gonocytes proliferate for a few days and then arrest in the G_0/G_1 phase until birth. Within a few days after birth, the gonocytes resume proliferation to initiate spermatogenesis. By day 6 postpartum, these cells migrate to the basement membrane of the seminiferous tubules and become undifferentiated type A spermatogonia, the male germline stem cells (*4*). Type A spermatogonia either renew themselves to maintain the pool of stem cells or undergo differentiation to produce spermatozoa (*5*). The male germline stem cell expresses high levels of telomerase activity, but during germ cell differentiation, telomerase activity is progressively lost (*6*). Furthermore, telomerase deficiency in mice leads to a depletion of male germ cells (*7*). Given the evidence that the ectopic expression of the telomerase catalytic component, TERT, in certain cell types can extend their life-span and even immortalize them (*8, 9*), it was suggested that spermatogonia may be maintained in an undifferentiated status by overexpression of TERT in vitro.

We created cell lines using undifferentiated type A spermatogonia obtained from 6-day-old BALB/c mice isolated by the STAPUT method (*10*). Because primary spermatogonia are difficult to transfect, we used a retrovirus system to introduce mTERT. The retrovirus construct was generated by inserting mTERT cDNA into the EcoR I site of the retrovirus vector pLXSN (*11*). Isolated cells were infected with the retrovirus following a standard protocol (*12*). After 2 months of culture in the presence of G418, the cells expanded as they became immortalized. Many of the cells displayed a morphology similar to primary type A spermatogonia, such as a large cell body and a spherical nucleus with a thin rim of cytoplasm and with perinuclear organelles (Fig. 1, A and B). Immunocytochemistry showed that the cells also expressed c-kit, which is a biochemical marker for spermatogonia (Fig. 1C). Six clones, S1 to S6, were obtained by subcloning from the immortalized mixed culture. After 1 year in culture, the cells (Fig. 1D) still displayed a morphology similar to that of freshly isolated type A spermatogonia and maintained the expression of telomerase, as shown by Northern blot (Fig. 1E). To further confirm the germ cell characteristics of these cells, we checked for Dazl, a germ cell–specific RNA-binding protein (*13*), and Oct-4, a germ cell–specific transcriptional factor (*14*). As shown by reverse-transcription polymerase chain reaction (RT-PCR) (*15*) and Western blot, all the cell lines were positive for both Oct-4 and Dazl (Fig. 1, F and G), respectively. Oct-4 is expressed in totipotent embryonic cells. After gastrulation, Oct-4 expression becomes restricted to PGCs. In male mice, the expression of Oct-4 is maintained until the beginning of spermatogenesis and is confined to the type A spermatogonia (*16*). Thus, these immortalized cells were likely derived from type A spermatogonia.

We further examined the physiological function of these cells by inducing differentiation with stem cell factor (SCF). In vivo, the type A spermatogonia go through several cycles of mitosis, forming many interconnected cells that enter meiosis (*17*). SCF and its receptor c-kit play a critical role in regulating this initial stage of spermatogenesis and trigger the proliferation/differentiation of type A spermatogonia (*18*). A point mutation in c-kit, which impairs SCF-mediated activation of phosphatidylinositol 3-kinase, leads to complete male sterility due to lack of differentiating spermatogonia (*19, 20*). All six cell lines demonstrated the presence of c-kit as shown by Western blot (Fig. 1H). We treated the S4 cells with mSCF to induce spermatogenesis in vitro. S4 cells responded to mSCF, as shown by tyrosine phosphorylation of c-kit within 5 min of mSCF (100 ng/ml) treatment (Fig. 1I).

We further analyzed the differential capacity of S4 cells to produce meiotic cells. The meiotic cell is distinguished from the mitotic cell by unique chromosome patterns,

[1]Department of Cell Biology, Georgetown University Medical Center, Washington, DC 20007, USA. [2]Department of Obstetrics, Gynecology, and Reproductive Sciences, University of California, San Francisco, CA 94143, USA. [3]Department of Cell Biology, University of Virginia School of Medicine, Charlottesville, VA 22908, USA. [4]Department of Biochemistry, Molecular Biology, and Cell Biology, Northwestern University, Chicago, IL 60208, USA.

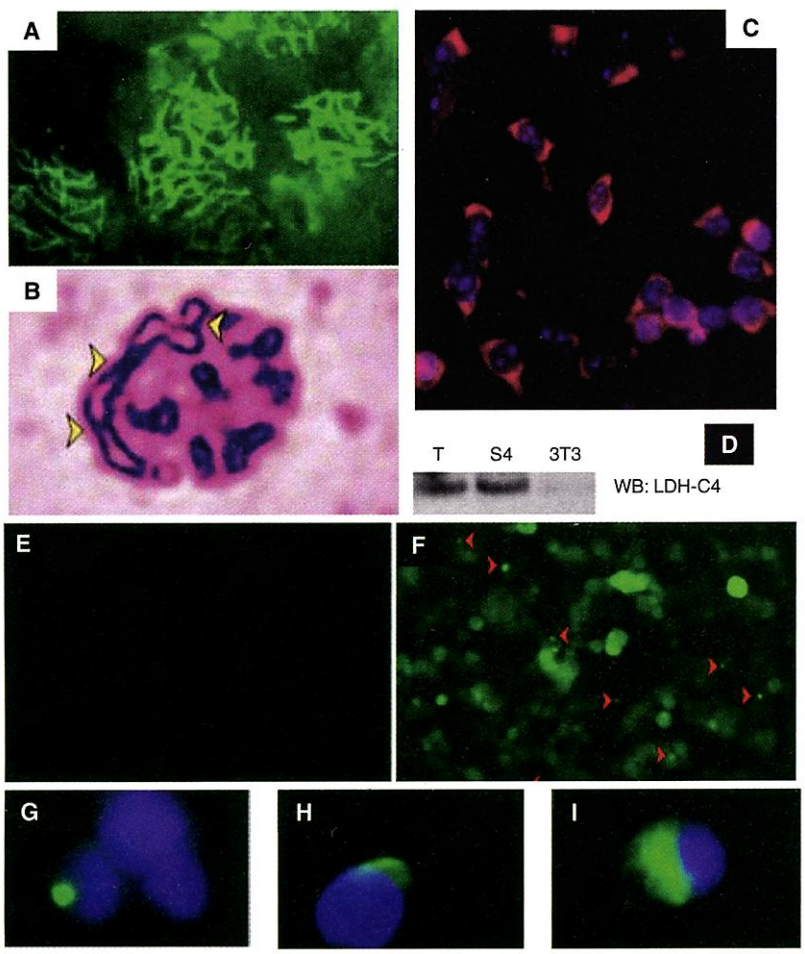

Fig. 2. Characterization of differentiated cells. (**A**) Synaptonemal complexes in S4 cells after 7 days of culture with mSCF (100 ng/ml), shown by immunofluorescence with antibody to SCP3. (**B**) Crossovers shown by Giemsa staining in induced S4 cells (arrowheads). (**C** and **D**) Immunocytochemistry and Western blot showing LDH-C4 expression in induced S4 cells. (**E**) Acr3-EGFP stably transfected S4 cells (control). (**F**) mSCF-induced Acr3-EGFP stably transfected S4 cells. The population of GFP-positive cells included large, round cells that are pachytene spermatocytes and round spermatids, which were smaller and showed a tiny green dot (red arrowheads), the proacrosomal granule. (**G** to **I**) Round spermatids stained with 4′,6′-diamidino-2-phenylindole (DAPI) (blue). Different stages of acrosome formation are shown by Acr3-EGFP (green).

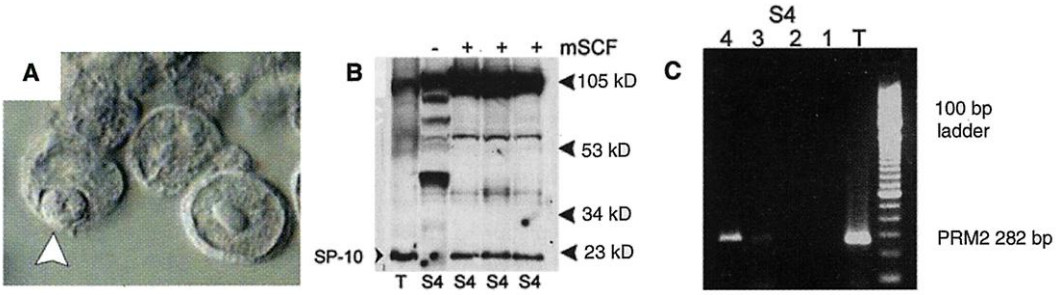

Fig. 3. (**A**) Differential interference contrast image showing a granule in a spermatid (arrowhead). (**B**) Western blot showing that SP-10 expression was induced by SCF; lane T is a control from adult testis. (**C**) RT-PCR for protamine-2 expression. Lane T, adult testis; lane 1, non-RT control for S4 cells after 3 weeks induction; lane 2, 1 week induction; lane 3, 2 weeks induction; lane 4, 3 weeks induction.

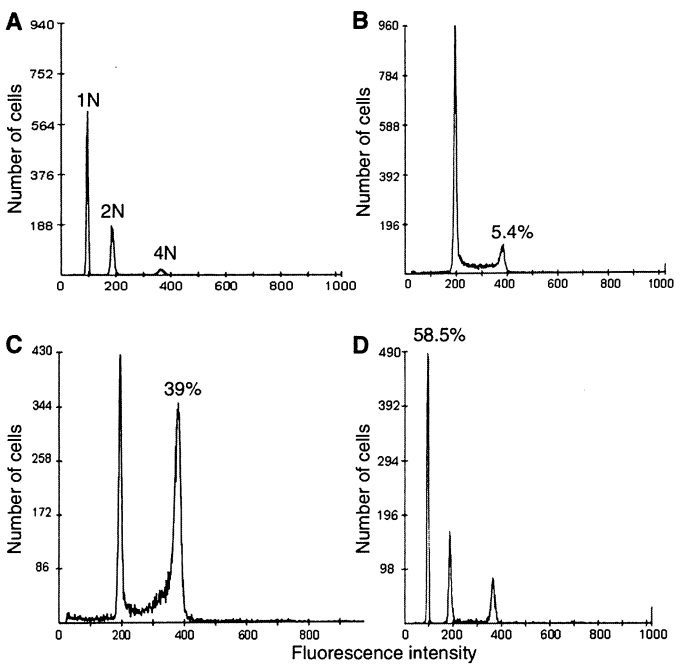

Fig. 4. Flow cytometry analysis. (**A**) Adult mice testes were digested and the cell mixture was fixed with 70% ethanol and stained with propidium iodide. DNA content was measured to show cell ploidy. (**B**) S4 cells before induction; the percentage of the 4N cell population is 5.4%. (**C**) After 1 week of induction with mSCF, 39% of the cells were 4N. (**D**) Haploid cells were produced at 58.5% of the total cell population after 3 weeks of SCF induction.

especially the assembly of the synaptonemal complex (SC) and the formation of chiasmata at the sites of crossover (genetic recombination). Immunofluorescence staining with an antibody to synaptonemal complex protein 3 (SCP3) revealed that mSCF induced the formation of SCs in the S4 cells within a week of culture (Fig. 2A). Moreover, crossovers also were found in the mSCF-induced meiotic S4 cells as shown by Giemsa staining (Fig. 2B). These SCF-induced cells were also strongly positive for the meiosis-specific marker lactate dehydrogenase (LDH-C4) (*21*) (Fig. 2, C and D).

After two meiotic divisions, spermatocytes give rise to haploid spermatids. We next used an Acr3-EGFP (enhanced green fluorescent protein) construct to test whether S4 cells differentiate into spermatids. Acr3-EGFP was made by inserting EGFP at the downstream site of a fused peptide of proacrosin signal fragment (MVEMLPTVAVLVLAVSVVA) and its N-terminal peptide (KDNTT) (*22*). The expression of the whole fusion protein is driven by the acrosin promoter. In Acr3-EGFP transgenic mouse lines, an accumulation of GFP was evident as tiny dots corresponding to proacrosomal granules at step 1 or 2 in spermatid differentiation. The green fluorescence merged to form one large granule and then flattened into a characteristic cap shape as spermiogenesis proceeded (*23*). The acrosin promoter is first activated in the cytoplasm of stage IV pachytene spermatocytes and then continues throughout the early stages of spermiogenesis (*24*). Thus, Acr3-EGFP can be used to identify both meiotic and postmeiotic cells after introduction into our cell line. The stably transfected S4 cells were created by introducing Xba I–linearized Acr3-EGFP-pcDNA3.1/Zeo(-) (*25*).

After SCF stimulation, both meiotic cells and postmeiotic cells were observed by GFP (Fig. 2, E and F). Some cells had a tiny green GFP dot at the cell pole, similar to what was seen in postmeiotic cells in the Acr3-EGFP transgenic mice. These cells appeared to be step 1 or step 2 round spermatids. Some of these cells differentiated into more mature spermatids (Fig. 2, G to I), although sperm tails were not evident. The formation of an acrosome in SCF-induced cells was also revealed by differential interference contrast microscopy (Fig. 3A). We further examined the expression of the spermatid-specific markers SP-10 (*26*) and protamine-2 (*27*) in the SCF-induced cell line. As shown by Western blot and RT-PCR (*15*), the cells expressed both SP-10 protein and protamine-2 after 2 weeks of stimulation with mSCF (Fig. 3, B and C).

Flow cytometry analysis was carried out to examine the number of chromosomes (ploidy) in the spermatogonial cell line. Spermatogonia contain the diploid (2N) number of chromosomes. As shown in Fig. 4B, the noninduced S4 cells are diploid and not aneuploid. Aneuploidy is the karyotype of transformed testicular cells (*28*). After 1 week of SCF induction, 39% of the S4 cells were tetraploid (4N), as is typical of spermatocytes (Fig. 4C). After 3 weeks of induction, the number of haploid cells (1N) reached 58.5% of the total cell population (Fig. 4D). Spermatids normally contain the 1N number of chromosomes. Thus, the S4 cells appear to differentiate into spermatocytes and round spermatids upon SCF stimulation. Figure 4A shows the ploidy from a normal testis.

It was previously reported that meiotic cells and spermatids were generated from a male germ cell line established by cotransfecting with the simian virus 40 (SV40) large tumor antigen gene and a mutant of p53 (*29*). However, a subsequent report by the same group could not confirm the original work (*30*). It is likely that the cell line was transformed. Although telomerase is highly expressed in most transformed cells, there is clear evidence that overexpression of TERT can immortalize cells without transformation (*8, 9*). TERT has been widely used to establish a number of cell lines (*31*). Our mTERT-immortalized mouse spermatogonial cells have the properties of type A spermatogonial stem cells because they can proliferate to renew themselves and can also give rise to differentiated cells upon ligand stimulation. Bridges have not been noted between the dividing or the differentiating cells; the role of the bridges in vivo still remains to be elucidated. This cell line can be used to examine mouse spermatogenesis in vitro at the molecular level. It also will be a useful model system to analyze the mechanisms of infer-

tility caused by genetic factors and drug toxicity.

Recently, transgenic mice were produced by retroviral transduction of male germline stem cells (*32*). However, the efficiency and the definition of integration of exogenous genes into the genome remain to be improved. It is very difficult to transfer genes into primary cultures of spermatogonia and impossible to select them with drugs in vitro. Use of the spermatogonial cell line may resolve current challenges with primary cultures of isolated spermatogonia and may greatly increase the success and efficiency of generating transgenic mice.

References and Notes

1. M. Starz-Gaiano, R. Lehmann, *Mech. Dev.* **105**, 5 (2001).
2. P. P. Tam, M. H. Snow, *J. Embryol. Exp. Morphol.* **64**, 133 (1981).
3. P. J. Donovan, D. Stott, L. A. Cairns, J. Heasman, C. C. Wylie, *Cell* **44**, 831 (1986).
4. A. McLaren, *Mol. Cell. Endocrinol.* **163**, 3 (2000).
5. M. Dym, *Proc. Natl. Acad. Sci. U.S.A.* **91**, 11287 (1994).
6. N. Ravindranath *et al.*, *Endocrinology* **138**, 4026 (1997).
7. H. W. Lee *et al.*, *Nature* **392**, 569 (1998).
8. W. C. Hahn *et al.*, *Nature* **400**, 464 (1999).
9. C. P. Morales *et al.*, *Nature Genet.* **21**, 115 (1999).
10. M. Dym *et al.*, *Biol. Reprod.* **52**, 8 (1995).
11. A 3441–base pair (bp) EcoR I/EcoR I fragment carrying 3395 bp of full-length murine telomerase reverse transcriptase (mTERT) cDNA was obtained from pGRN188 and subcloned into EcoR I site in a retrovirus vector pLXSN (Clontech). The orientation for expressing sense mTERT by 5′ LTR was checked by digestion with Xho I. Expression of Neo^r was driven by SV40 early promoter. Viruses were harvested from supernatants of transfected Phoenix packaging cells.
12. W. S. Pear *et al.*, *Proc. Natl. Acad. Sci. U.S.A.* **90**, 8392 (1993).
13. M. Ruggiu *et al.*, *Nature* **389**, 73 (1997).
14. H. R. Schöler, S. Ruppert, N. Suzuki, K. Chowdhury, P. Gruss, *Nature* **344**, 435 (1990).
15. Total RNA was isolated and cDNA synthesis was carried out with random hexamers. RT-PCR amplification of Oct-4 used primers 5′-AGCTGCTGAAGCAGAAGAGG-3′ and 5′-GGTTCTCATTGTTGTCGGCT-3′ (94°C for 35 s, 55°C for 30 s, and 72°C for 45 s; 30 cycles). The size of the RT-PCR product was 207 bp. Primers for RT-PCR amplification of protamine-2 were 5′-GAGCGCGTAGAGGACTATGG-3′ and 5′-GCAAGTGACTTCCTTGGCTC-3′ (94°C for 30 s, 58°C for 30 s, and 72°C for 45 s; 35 cycles). The product was a 282-bp DNA fragment.
16. M. Pesce, M. K. Gross, H. R. Schöler, *Bioessays* **20**, 722 (1998).
17. D. G. de Rooij, J. A. Grootegoed, *Curr. Opin. Cell Biol.* **10**, 694 (1998).
18. H. Ohta, K. Yomogida, K. Dohmae, Y. Nishimune, *Development* **127**, 2125 (2000).
19. P. Blume-Jensen *et al.*, *Nature Genet.* **24**,157 (2000).
20. H. Kissel *et al.*, *EMBO J.* **19**, 1312 (2000).
21. Z. G. Liang, J. A. Shelton, E. Goldberg, *J. Exp. Zool.* **240**, 377 (1986).
22. Single-letter abbreviations for amino acid residues are as follows: A, Ala; C, Cys; D, Asp; E, Glu; F, Phe; G, Gly; H, His; I, Ile; K, Lys; L, Leu; M, Met; N, Asn; P, Pro; Q, Gln; R, Arg; S, Ser; T, Thr; V, Val; W, Trp; and Y, Tyr.
23. T. Nakanishi *et al.*, *FEBS Lett.* **449**, 277 (1999).
24. S. Kashiwabara, Y. Arai, K. Kodaira, T. Baba, *Biochem. Biophys. Res. Commun.* **173**, 240 (1990).
25. Acr3-EGFP-pcDNA3.1/Zeo(-) was created by subcloning the Xba I/Hind III fragment of Acr3-EGFP [containing acrosin promoter, the fused peptide MVEMLPTVAVLVLAVSVVA-KDNTT-EGFP (*22*), and bovine growth hormone polyadenylate from pUC19/Acr3-EGFP] into pcDNA3.1/Zeo(-).
26. P. P. Reddi, C. J. Flickinger, J. C. Herr, *Biol. Reprod.* **61**, 1256 (1999).
27. P. Mali *et al.*, *Reprod. Fertil. Dev.* **1**, 369 (1989).
28. X. Meng *et al.*, *Cancer Res.* **61**, 3267 (2001).
29. M. C. Hofmann, R. A. Hess, E. Goldberg, J. L. Millan, *Proc. Natl. Acad. Sci. U.S.A.* **91**, 5533 (1994).
30. M. J. Wolkowicz *et al.*, *Biol. Reprod.* **55**, 923 (1996).
31. T. R. Yeager, R. R. Reddel, *Curr. Opin. Biotechnol.* **10**, 465 (1999).
32. M. Nagano *et al.*, *Proc. Natl. Acad. Sci. U.S.A.* **98**, 13090 (2001).

33. We thank M. Okabe for pUC19/Acr3-EGFP, P. Moens for antibody to SCP3, and R. A. DePinho for pGRN188. Supported in part by NIH grant HD-36483.

22 April 2002; accepted 12 June 2002
Published online 20 June 2002;
10.1126/science.1073162
Include this information when citing this paper.

Systematic Identification of Pathways That Couple Cell Growth and Division in Yeast

Paul Jorgensen,[1,2]* Joy L. Nishikawa,[1,2]* Bobby-Joe Breitkreutz,[2] Mike Tyers[1,2]†

Size homeostasis in budding yeast requires that cells grow to a critical size before commitment to division in the late prereplicative growth phase of the cell cycle, an event termed Start. We determined cell size distributions for the complete set of ~6000 *Saccharomyces cerevisiae* gene deletion strains and identified ~500 abnormally small (*whi*) or large (*lge*) mutants. Genetic analysis revealed a complex network of newly found factors that govern critical cell size at Start, the most potent of which were Sfp1, Sch9, Cdh1, Prs3, and Whi5. Ribosome biogenesis is intimately linked to cell size through Sfp1, a transcription factor that controls the expression of at least 60 genes implicated in ribosome assembly. Cell growth and division appear to be coupled by multiple conserved mechanisms.

Size homeostasis, whereby cell growth is coupled to cell division, is a universal but poorly understood feature of cell cycle control (*1*). In the budding yeast *S. cerevisiae*, coordination of division with growth occurs at Start, where cells must reach a critical cell size to enter the cell cycle (*2–4*). This size threshold increases in proportion to cell ploidy and nutrient status (*5, 6*). In fission yeast, unicellular algae, mouse fibroblasts, and human lymphoid cells, entrance into the DNA replication phase of the cell cycle (S phase) also requires that cells obtain a critical cell volume, as modulated by ploidy and extracellular signals (*7–11*). Recently, a signaling pathway comprising phosphoinositide-3′-kinase, the phosphoinositide phosphatase PTEN, Akt/protein kinase B (PKB), and ribosomal S6 kinase (S6K) has been implicated in cell size control in flies and mice (*1, 12–14*).

Mutations that accelerate cell division relative to cell growth result in a small cell size, referred to as a Wee or Whi phenotype in fission yeast and budding yeast, respectively. Such mutants have provided key insights into cell cycle control (*7, 15–18*). Two *whi* mutants, *WHI1-1* (or *CLN3-1*) and *whi3*, have a reduced critical cell size at Start. *WHI1-1* is a hypermorphic allele of *CLN3*, which encodes a cyclin that activates the cyclin-dependent kinase Cdc28 to cue events at Start (*15–17, 19*), whereas Whi3 is an RNA binding protein that sequesters the *CLN3* transcript into an inactive state (*18, 20*). In the late prereplicative growth phase of growth (G_1), the Cln3-Cdc28 kinase and another protein of unknown function, Bck2, impel the SCB binding factor (SBF) (Swi4-Swi6) and MCB binding factor (MBF) (Mbp1-Swi6) transcription factor complexes to drive the expression of a suite of ~120 genes, including the G1 cyclins *CLN1* and *CLN2* (*19, 21–23*). Cln1-Cdc28 and Cln2-Cdc28 activity triggers key events at Start, including bud emergence, spindle pole body duplication, and elaboration of Clb-Cdc28 activity, which is needed for DNA replication (*3*).

Despite the insights gleaned from analysis of *whi* mutants, few such mutants have been characterized because of the difficulties inherent in cloning genes that affect cell size (*16*). The recent construction of a complete set of yeast open reading frame (ORF) deletion strains allowed us to survey 4812 viable haploid deletion strains for alterations in the cell size distributions of exponentially grow-

[1]Department of Medical Genetics and Microbiology, University of Toronto, Toronto, Ontario, Canada M5S 1A8. [2]Program in Molecular Biology and Cancer, Samuel Lunenfeld Research Institute, Mount Sinai Hospital, Toronto, Ontario, Canada M5G 1X5.

*These authors contributed equally to this work.
†To whom correspondence should be addressed. E-mail: tyers@mshri.on.ca